

## **SUPPORTING INFORMATION**

### **A Multifunctional Thermochromic-Elastomeric Composite for Integrated Pressure and Temperature Sensing**

*Fatemeh Motaghedi,<sup>1</sup> Lina Rose,<sup>1,2</sup> Mohammed Jalal Ahamed,<sup>2\*</sup> Tricia Breen Carmichael<sup>1,\*</sup> and Simon Rondeau-Gagné<sup>1,\*</sup>*

<sup>1</sup> Department of Chemistry and Biochemistry, University of Windsor, Ontario, Canada N9B 3P4

<sup>2</sup> Department of Mechanical, Automotive and Materials Engineering, University of Windsor, Ontario, Canada N9B 3P4

\* Prof. Simon Rondeau-Gagné ([srondeau@uwindsor.ca](mailto:srondeau@uwindsor.ca))

\* Prof. Tricia Breen Carmichael ([tbcarmic@uwindsor.ca](mailto:tbcarmic@uwindsor.ca))

\* Prof. M. Jalal Ahamed ([M.Ahamed@uwindsor.ca](mailto:M.Ahamed@uwindsor.ca))

#### **Table of Contents**

|  |            |
|--|------------|
| - Material and Instruments .....             | <b>S2</b>  |
| - Device Fabrication .....                   | <b>S3</b>  |
| - Device and Materials Characterization..... | <b>S4</b>  |
| - References .....                           | <b>S10</b> |

## Instruments

Fourier-transform Infrared (FT-IR) spectroscopy was performed using a Bruker Alpha spectrometer. Confocal Raman spectroscopy was carried out using a WiTec Raman system equipped with a 1064 nm laser source processed using Project FOUR 4.0 software. UV-vis spectroscopy was performed on a Varian UV/Visible Cary 50 spectrophotometer. The MAP patterns were created using 3D printed molds, which were designed in SolidWorks and fabricated on a Creality Ender-3 3D printer (fused deposition modeling) with PLA filament, printed at 100% infill. Electrodes were fabricated by spray-coating a CNT solution to form the conductive layer. A Timber tech airbrush compressor equipped with a 0.2 mm needle nozzle was used for spraying at an operating pressure of about 20 psi. The setup included a compressor linked to the airbrush gun via an air hose. During the process, the air pressure was regulated at around 15 psi to ensure uniform and smooth deposition of the solution. Electrical characterization like capacitance measurements of the patterned dielectric structures and sensors were performed using a KEYSIGHT E4980AL LCR meter. Mechanical loading tests were carried out with a MARK-10 force gauge and calibrated weights ranging from 10 g to 500 g. Tensile behavior was studied using a micrometer-controlled stretching apparatus with a Velmex slide stage, while Young's modulus was determined with an INSTRON tensile testing machine. For these tests, the samples were cast in dog-bone-shaped PTFE molds (35 mm length, 17 mm width, 2 mm thickness). The crosshead speed was set to 2 mm/s, and the resulting load (in kN) was recorded at each displacement step.

## Device Fabrication

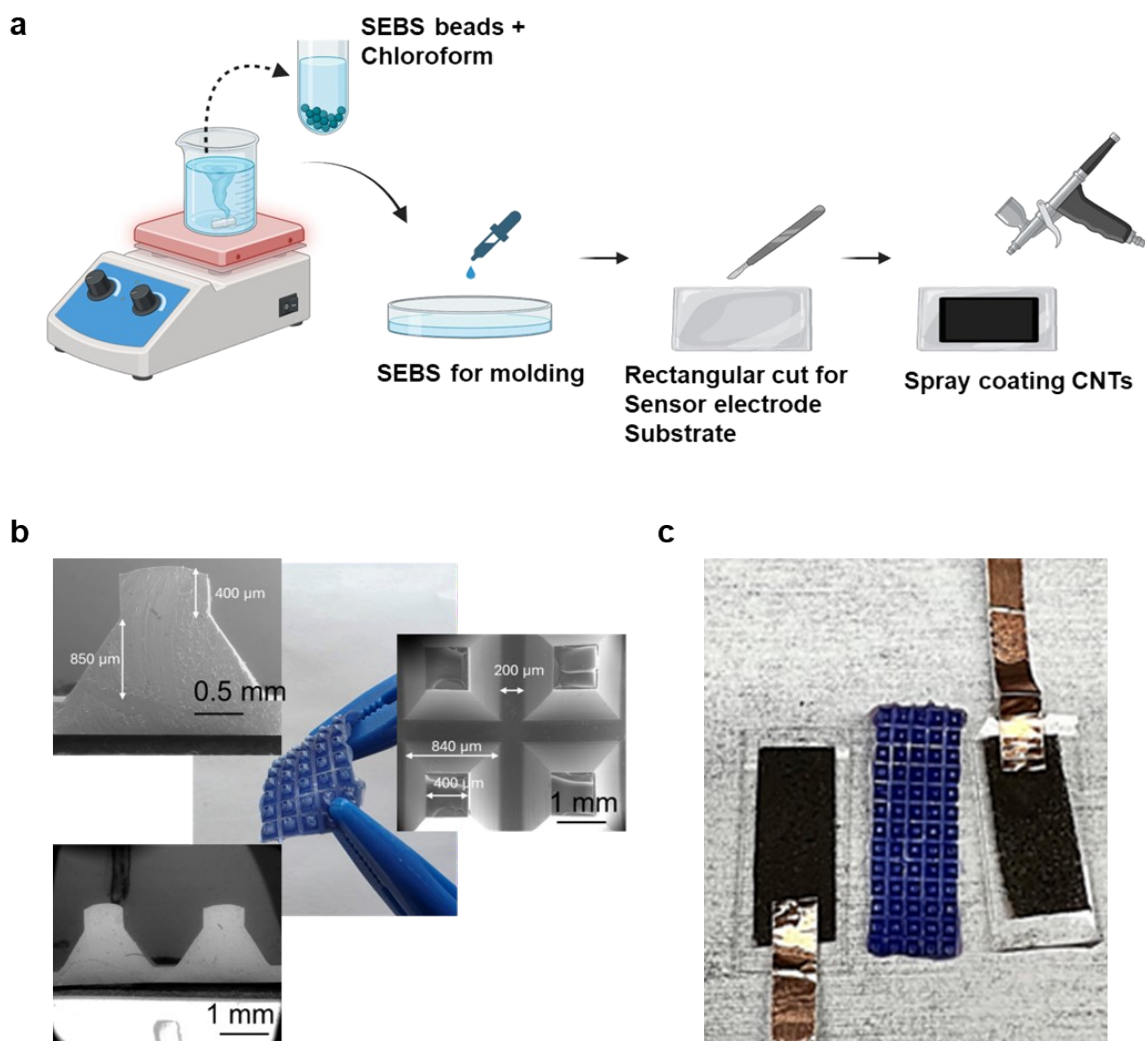


**Figure S1.** a) Fabrication process for the electrode; b) scanning-electron microscopy (SEM) image of SEBS-PDA-MAP, and c) image of the sensor with SEBS-PDA-MAP dielectric.

## Device and Materials Characterization

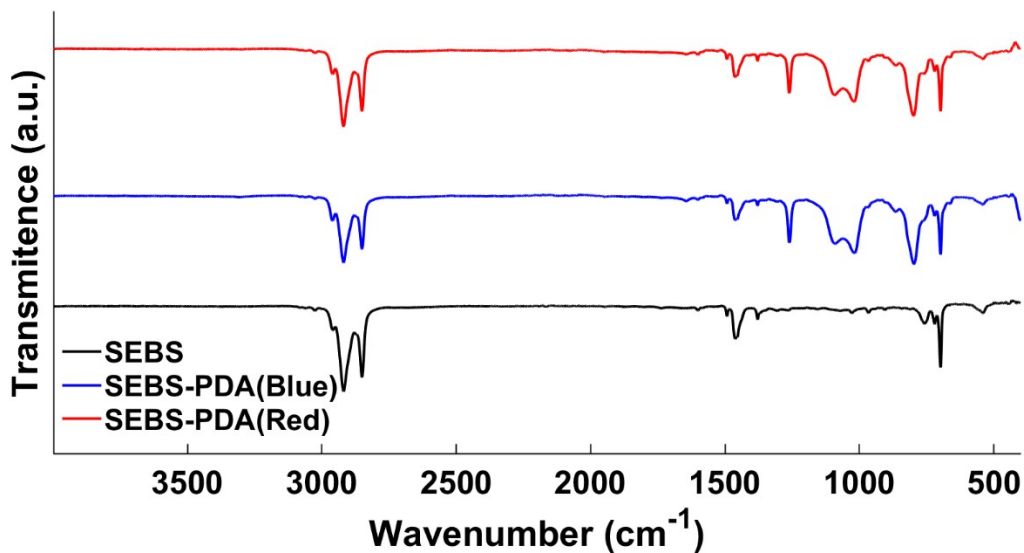


**Figure S2.** FTIR spectra of SEBS film and SEBS-PDA composite film at room temperature (blue phase) and heated at 60°C (red phase).

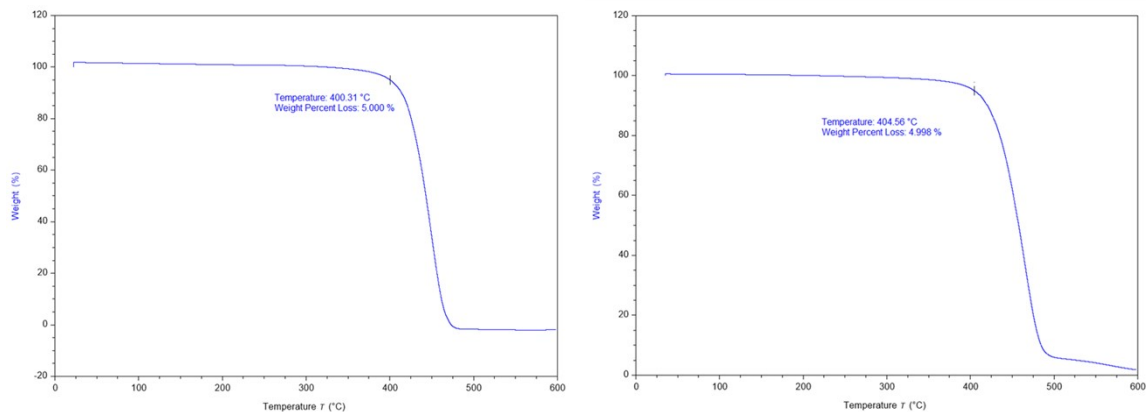


**Figure S3.** Thermogravimetric analysis (TGA) of pure SEBS (*left*) and SEBS-PDA composite (*right*).

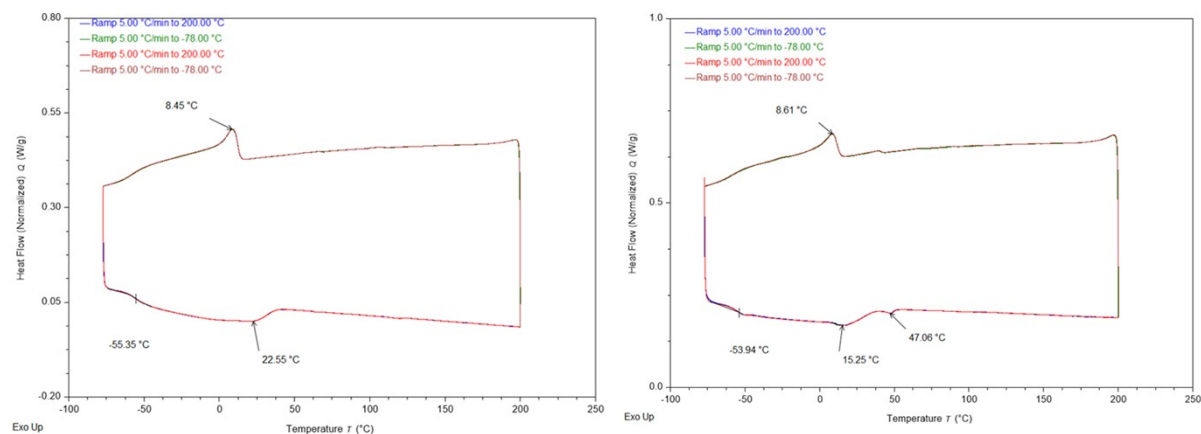


**Figure S4.** Differential scanning calorimetry (DSC) thermograms of SEBS (*left*) and SEBS-PDA composite (*right*).

**Table S1** Comparison of pressure sensitivity of SEBS–PDA MAP and PDMS-MAP sensors

| Parameter                            | SEBS-PDA-MAP           | PDMS-MAP                |
|--------------------------------------|------------------------|-------------------------|
| Sensitivity at start of fatigue test | 60 kPa <sup>-1</sup>   | 76.69 kPa <sup>-1</sup> |
| Sensitivity after fatigue tests      | 63.8 kPa <sup>-1</sup> | 66 kPa <sup>-1</sup>    |
| Response time                        | 0.54 sec               | 0.19 sec                |

**Table S2.** Comparison of key characteristics of selected soft pressure sensors

| Sensing Materials  | Sensitivity (kPa <sup>-1</sup> ) | Response time (Sec) | Reference        |
|--------------------|----------------------------------|---------------------|------------------|
| PDMS               | 76.7                             | 0.19                | 1                |
| WCNT/PEDOT:PSS     | 10.8                             | 0.12                | 2                |
| PDMS               | 0.040                            | 94.0                | 3                |
| SEBS-PDA composite | 60.0                             | 0.54                | <b>This work</b> |

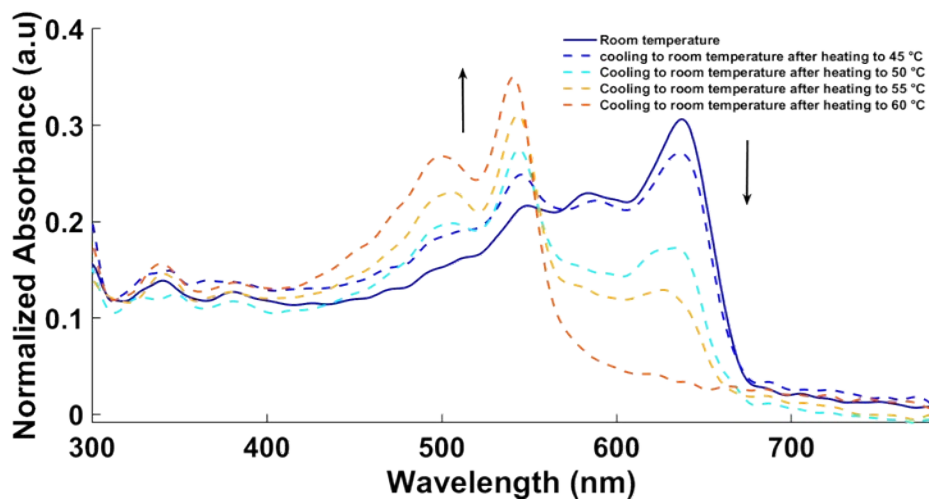


**Figure S5.** UV-vis spectra of the composite made from PDA-crosslinked PDMS in SEBS.

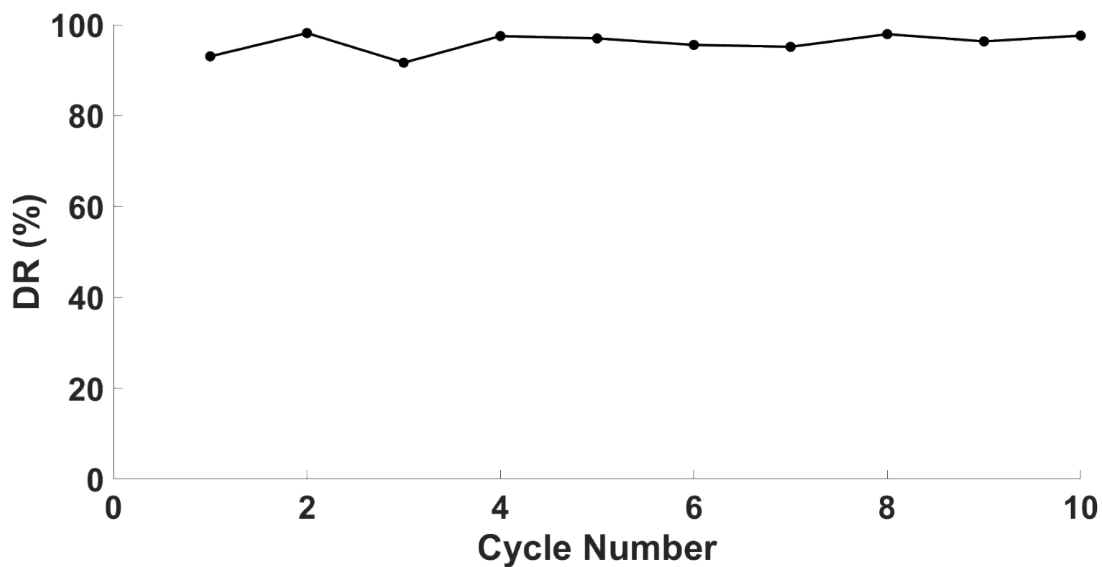


**Figure S6.** Degree of reversibility percentage of the thermochromic materials over 10 heating/cooling cycles between 25 to 45°C.

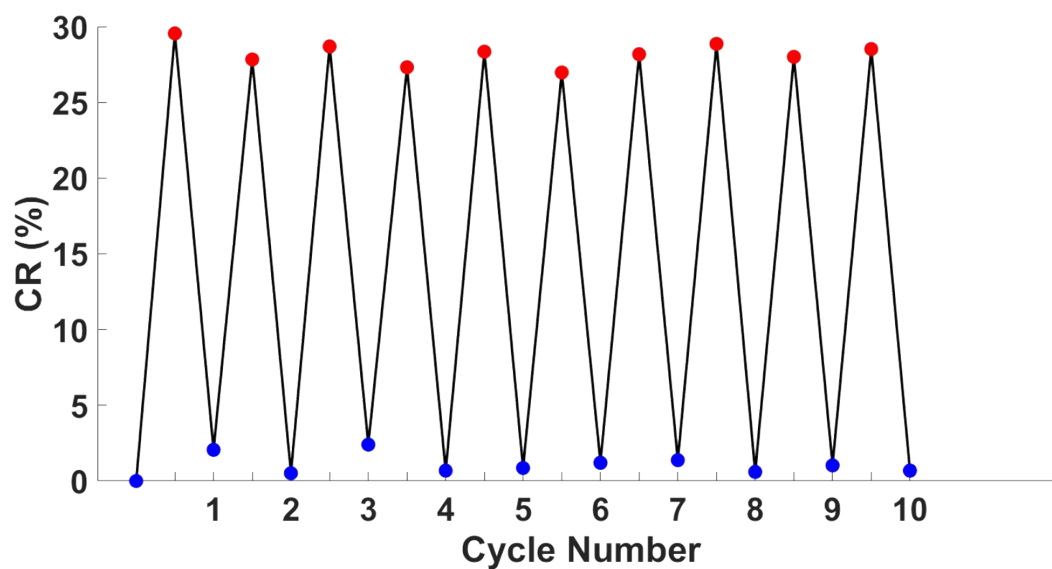


**Figure S7.** Colorimetric response percentage over 10 heating/cooling cycles between 25 to 45°C

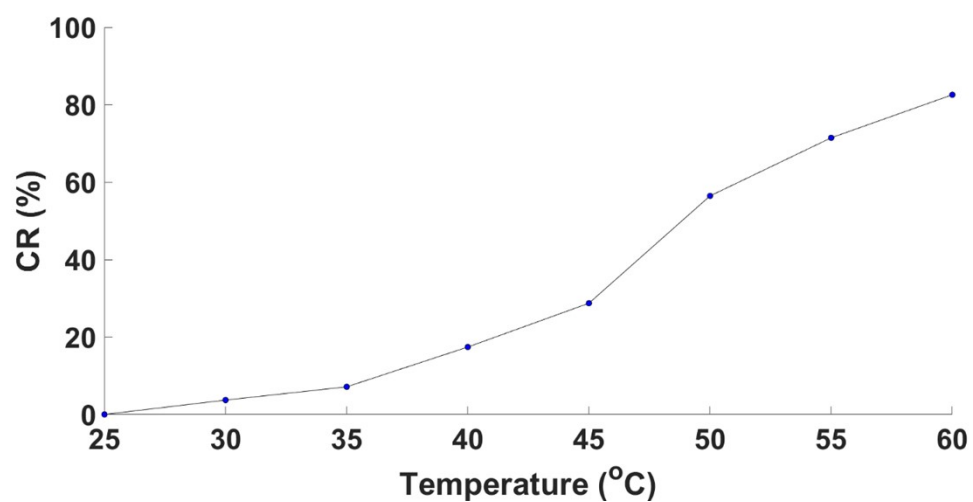


**Figure S8.** Colorimetric response percentage of PDA-crosslinked PDMS films from 25 - 60 °C.

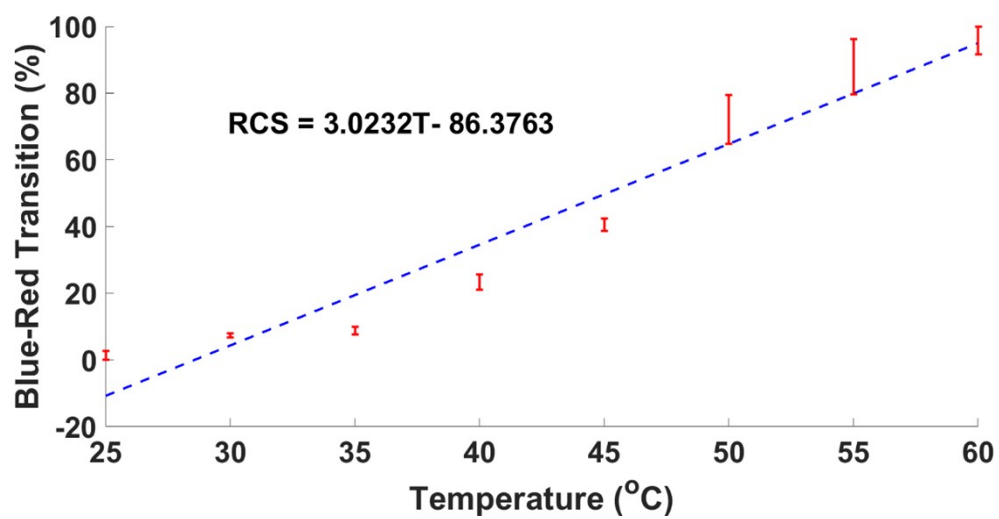


**Figure S9.** Colorimetric response percentage of PDA-crosslinked PDMS in SEBS-PDA films from 25 - 60 °C.



**Figure S10.** SEBS-PDA film after heating beyond 90 °C.



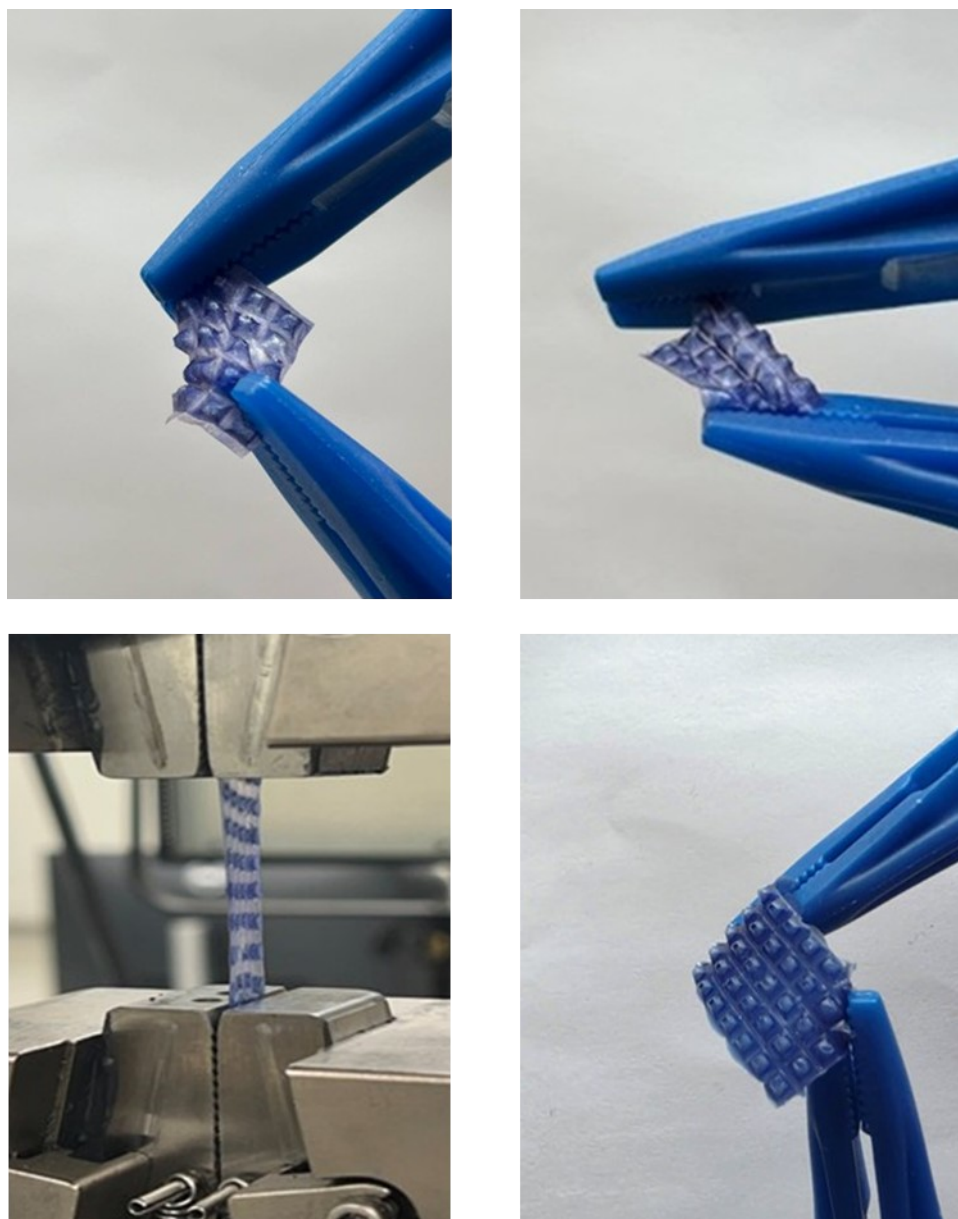


**Figure S11.** Free-standing tensile tests of the SEBS–PDA composite showing no observable color change upon stretching. Repeated mechanical deformation using tweezers similarly did not induce any detectable optical shift.

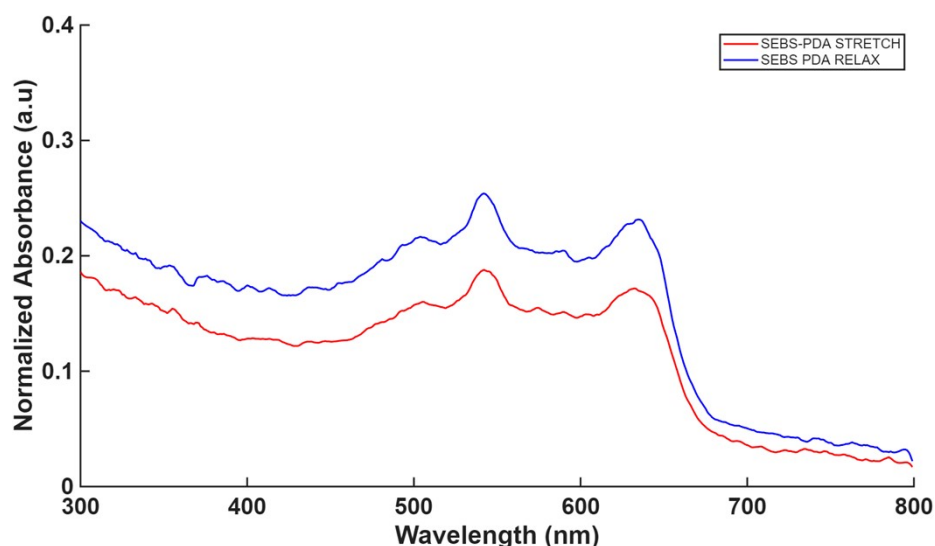


**Figure S12.** UV-vis spectroscopy of SEBS-PDA composite (blue phase) upon stretching (red) and without tensile strain (blue).

## References

- 1 L. Rose, G. Nagesh, P. Das, D. Skaf, F. Motaghedi, S. Rondeau-Gagné and M. J. Ahamed, Exploring mesoamerican pyramidal micro-structures in soft capacitors for positive and negative pressure sensing, *Flex. Print. Electron.*, 2025, **10**, 025003.
- 2 Z. Chen, S. Liu, P. Kang, Y. Wang, H. Liu, C. Liu and C. Shen, Decoupled Temperature–Pressure Sensing System for Deep Learning Assisted Human–Machine Interaction, *Adv. Funct. Mater.*, 2024, **34**, 2411688.
- 3 S. Liu, X. Yue, S. Liu, W. Yang, H. Liu, C. Liu and C. Shen, Deep learning-assisted tactile sensing platform for efficient object classification and password recognition, *J. Mater. Sci. Technol.*, 2026, **260**, 241–252.